



Contents lists available at ScienceDirect

Bioorganic & Medicinal Chemistry Letters

journal homepage: www.elsevier.com/locate/bmcl

A mitochondria-selective near-infrared-emitting fluorescent dye for cellular imaging studies

Peter Choi^a, Katsuya Noguchi^b, Munetaka Ishiyama^b, William A. Denny^a, Jiney Jose^{a,*}

^a Auckland Cancer Society Research Centre, School of Medical Sciences, University of Auckland, Private Bag 92019, Auckland, 1142, New Zealand

^b Dojindo Laboratories Co., Ltd, Techno-Research Park Tabaru 2025-5 Mashiki-machi, Kamimashiki-gun, 861-2202, Japan

ARTICLE INFO

Article history:

Received 23 January 2018

Revised 26 April 2018

Accepted 1 May 2018

Available online xxxxx

Keywords:

Near infrared fluorescent dyes

Mitochondria

Amoxapine

Cyanine dye

Organelle selective fluorescent dyes

ABSTRACT

This communication details the synthesis, evaluation of photophysical properties, and cellular imaging studies of cyanine chromophore based fluorescent dye **1** as a selective imaging agent for mitochondria.

© 2018 Elsevier Ltd. All rights reserved.

Introduction

Organelle selective fluorescent probes are useful tools for delineating functional and morphological changes of various organelles, especially in a diseased state.¹ There are number of such probes reported in the literature, exemplifying the detailed synthetic efforts various groups have put in over the years to make them available to the scientific community.^{2–4} These probes are biocompatible, nontoxic and mostly selective towards their target.⁵ Although much work has been accomplished with molecules emitting in the 400–600 nm range, there still exists an opportunity to fine tune their emission towards the near infrared region (700–1000 nm) wherein there is minimal back ground fluorescence due to absorbing cellular entities and much greater tissue penetration. There is also minimal tissue damage caused by photons in this region of the spectrum.

An ongoing research project in our group focuses on developing organelle selective fluorescent probes for studying disease initiation at a cellular level. As our understanding of disease progression continues to advance it is becoming increasingly clear that certain organelles undergo changes during the onset of disease. Among them are mitochondria, the organelles responsible for energy production for various cellular functions, which have a major role associated with disease onset.⁶ Mitochondria are often referred to as the powerhouse of mammalian cells as they produce ATP

by a process called oxidative phosphorylation. Any defect in this pathway of ATP production will inevitably affect the cellular functions and ultimately lead to various disorders.⁷ Mitochondrial malfunction is associated with many diseases such as cancer, arthritis and heart disease.⁸

We have chosen to work with the cyanine scaffold due to its ease of synthetic manipulation and the subsequent fluorescence shift that can be achieved towards longer wavelength.⁹ In general, straight chain polymethine cyanine dyes suffer from photo stability issues due to photo oxidation caused by reactive oxygen species in aqueous media, which has hampered their widespread use as a class of dyes in biological conditions.¹⁰ However, their photo stability can be improved by introducing a cyclohexenyl ring as part of the polymethine chain.¹¹ IR-786 is one such heptamethine cyanine dye, incorporating a cyclohexenyl ring with a *meso*-chloro group which serves as a suitable electrophile to undergo reaction with various nucleophiles. There are many examples in the literature where the reactive chloro group is utilized to append various nucleophiles to modulate fluorescence properties which can then be used to monitor cellular processes and pH changes in cellular environment.^{12–14}

Fluorescent dyes have also been used to develop fluorescently tagged drug molecules in order to study the interaction of drugs with various receptor targets at the cellular level.¹⁵ One advantage of such a strategy is the ability to delineate the specific or non-specific interaction of a drug with various receptors which could then be used to improve the efficacy of the drug. Development of drugs targeting G-protein coupled receptors for therapeutic

* Corresponding author.

E-mail address: j.jose@auckland.ac.nz (J. Jose).

intervention is a good example which has benefited significantly using this strategy.¹⁶ The use of such strategy will greatly benefit the CNS drug discovery programme, where a lack of understanding of mechanism of action has to some extent hindered the treatment of neurodegenerative disorders such as Alzheimer's, Parkinson's and major depressive disorder (MDD).¹⁷

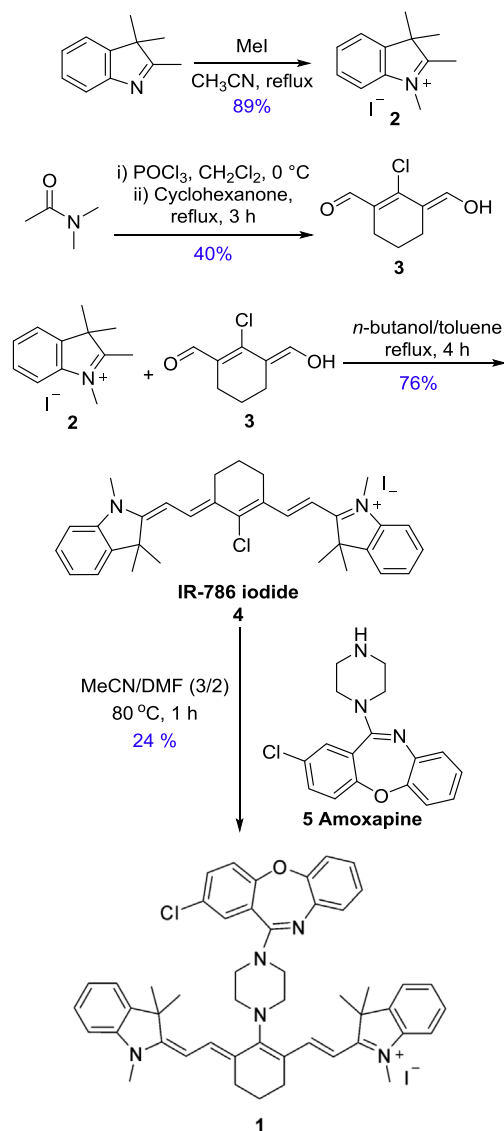
Amoxapine (2-chloro-11-(piperazin-1-yl)dibenzo[*b,f*][1,4]oxazepine) **5** (Scheme 1) is a tricyclic dibenzoxazepine antidepressant widely used in the treatment of MDD.¹⁸ Compared to other antidepressants it has a faster onset of action which makes it preferable for use in patients suffering from MDD. **5** is a known GUS (beta-glucuronidase) inhibitor which is used in combination with cytotoxic drugs to reduce drug side effects and improve potency. For example, the widely used colon and non-small cell lung cancer drug Irinotecan has the side-effect of severe diarrhoea. A combination of Irinotecan and **5** in animals have shown to completely alleviate diarrhoea and improve the potency of Irinotecan.¹⁹ **5** is also known to disrupt the mitochondrial electron transport chain which leads to metabolic acidosis and brain damage in patients.²⁰

To the best of our knowledge there are no literature reports of a near infrared dye attached to Amoxapine to study its mitochondrial selectivity. We therefore synthesized the Amoxapine-IR-786

dye **1** and were pleased to find that it was indeed selective towards mitochondria.

The synthesis of dye **1** is detailed in Scheme 1. IR-786 iodide **4** was first synthesized following a published procedure.²¹ Reaction between 2,3,3-trimethyl-3*H*-indole with methyl iodide²² yielded 1,2,3,3-tetramethyl-3*H*-indol-1-ium iodide **2** which was refluxed with (*E*)-2-chloro-3-(hydroxymethylene)cyclohex-1-ene-1-carbaldehyde **3** in *n*-butanol:toluene mixture for 4 h. Evaporation of the solvent, trituration of the crude solid material in methanol followed by filtration afforded IR-786 iodide **4** as green solid in 76% yield. Reaction of Amoxapine **5** with IR-786 iodide **4** in acetonitrile:DMF (3:2) at 80 °C for 1 h followed by flash silica chromatography (elution with 3% MeOH/DCM and trituration in hexanes) afforded dye **1** in 24% yield as a blue solid. The optimal Amoxapine **5**:IR-786 iodide **4** ratio for the reaction was found to be 5:1. Higher temperature and reaction time longer than 1 h resulted in lower yields presumably due to the instability of IR-786 iodide **4** to prolonged heating at higher temperature. All dyes were stored in the dark at -5 °C to avoid light induced decomposition.

The absorption and emission spectra of dye **1** and IR-786 iodide **4** were measured in ethanol (Fig. 1). The absorption and emission



Scheme 1. Synthesis of dye **1**.

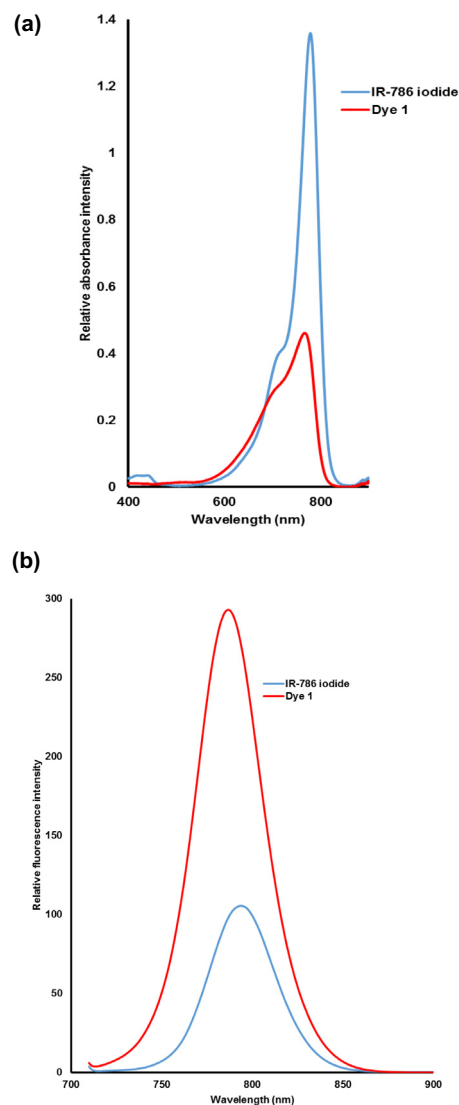


Figure 1. Relative absorbance (a) and fluorescence (b) intensity of IR-786 iodide **4** and dye **1** in EtOH. Concentration: 0.5 μ M. Dyes were excited at their respective absorption maxima.

of dye **1** shows a hypsochromic shift with respect to IR-786 iodide **4**. The absorption intensity of dye **1** is approximately threefold less than IR-786 iodide **4** whereas the fluorescence intensity is approximately threefold greater than that of **4**. The enhanced fluorescence intensity could be attributed to lesser degree of fluorescence quenching of dye **1** in ethanol as the structural modification prevents formation of aggregates. The full width at half maxima for both dyes are very similar. The quantum yield of dye **1** shows a 20% improvement over IR-786 iodide **4** (Table 1). Presence of Amoxapine **5** moiety enhances the solubility of dye **1** in ethanol and therefore presumably improves the quantum yield. The Stokes shift, the difference between the absorption and emission maxima for dye **1** is 21 nm compared to 16 nm for IR-786 iodide **4**. The molar extinction coefficient of Dye **1** is 3.5 times lower than that of IR-786 iodide **4**. The presence of Amoxapine **5** in the dye structure influences the absorption properties of the dye. Efficient bio imaging dyes should possess cell membrane penetrability, organelle selectivity, appreciable fluorescence in the near infra-red region to avoid back ground fluorescence, high molar extinction coefficient, sufficient aqueous solubility and stability. Dye **1** satisfies these criteria and therefore amenable for cellular imaging studies.

Fig. 2 shows the fluorescence images of HeLa cells incubated with Dye **1** and IR-786 iodide **4**. Dye **1** shows selective staining of mitochondria, whereas IR-786 iodide **4**, which is also cell permeable, does not show selectivity towards any organelles. Moreover, dye **1** appears significantly brighter compared to IR-786 iodide **4**, proving its utility as a useful cellular stain. The mitochondrial selectivity of dye **1** was confirmed by co-incubation of dye **1** with commercially available mitochondrial stains MitoTracker Green and MitoTracker Red (Fig. 3 and Supporting Information Figure S1). There appears to be a clear overlap of dye **1** fluorescence with that of MitoTracker Green and MitoTracker Red. The selectivity of the dye **1** towards mitochondria could be attributed to the lipophilic nature of the dye that assists with passage through the membrane and the delocalized positive charge helps the dye to target the interior of the mitochondria, which is negatively charged.

In order to study the mitochondrial membrane depolarization effect of dye **1**, HeLa cells were incubated with dye **1** and commercially available membrane permeant cyanine dye JC-1²³ which preferentially accumulates in mitochondria. JC-1 fluoresces red in normal polarized mitochondria and green in mitochondria which is depolarized or under stress. The decrease in red/green fluorescence intensity is indicative of mitochondrial depolarization.

Table 1
Photophysical properties of dyes in EtOH.

Dyes	Abs (nm)	Emiss (nm)	Stokes shift (nm)	ϵ (Mol ⁻¹ cm ⁻¹)	Quantum yield ^a	FWHM ^b
IR-786 iodide 4	778	794	16	271,600	0.031	43
Dye 1	766	787	21	77,400	0.038	43.5

^a Cyanine Cy5 in EtOH (ϕ :0.3 in Ethanol) used as a standard.

^b Fwhm: full width at half maximum for the fluorescence band.

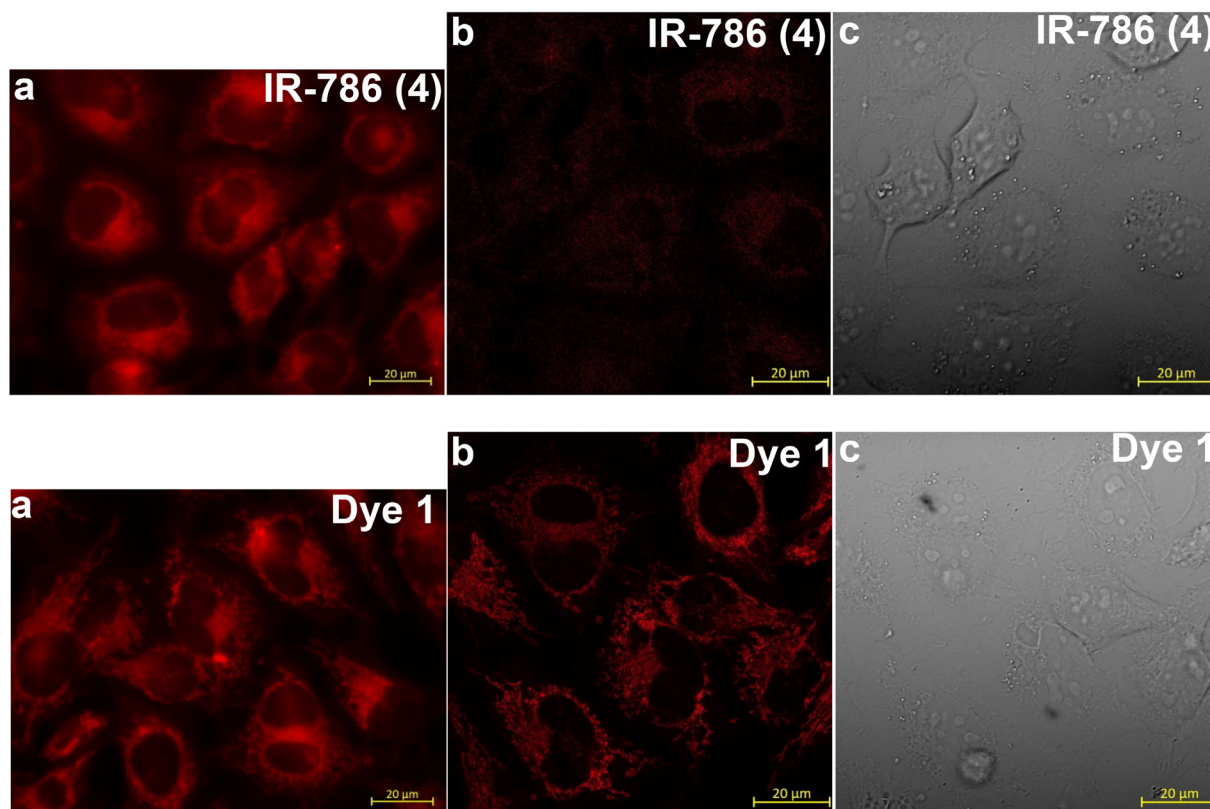


Figure 2. Epifluorescence (a), Confocal (b), Differential interference contrast (c) images of HeLa cells labelled with IR-786 iodide **4** (top row) and Dye **1** (bottom row). Scale bar: 20 μm.

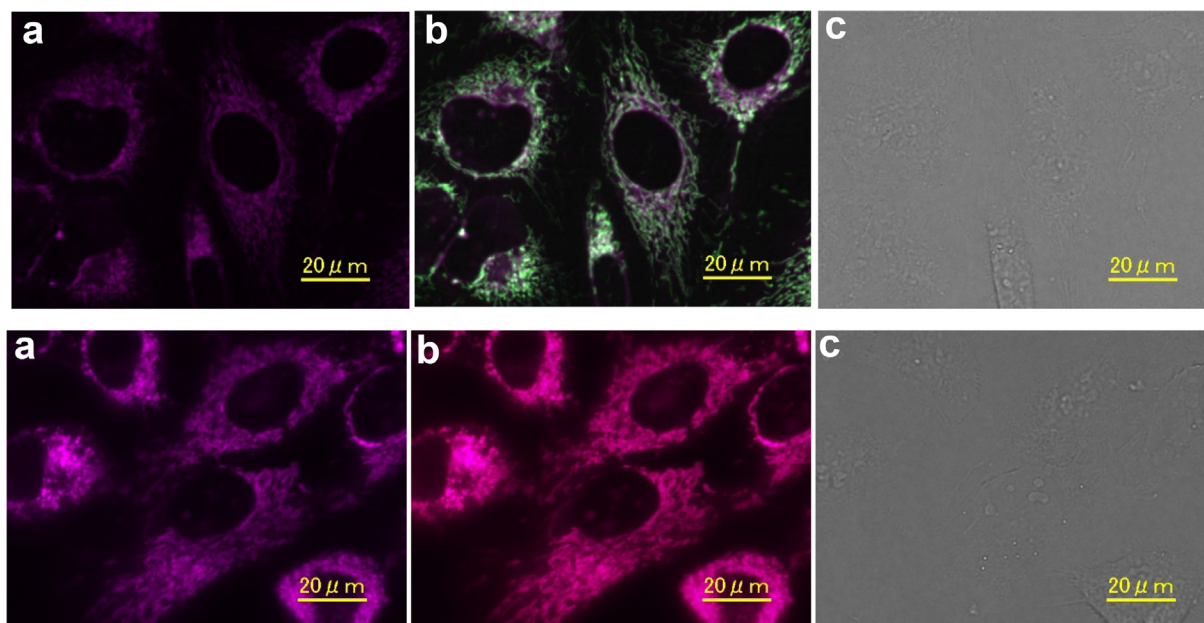


Figure 3. Dye **1** localized in Mitochondria (a) Dye **1** and MitoTracker Green (top)/Mito Tracker Red (bottom) co-localized in mitochondria (b) and differential interference contrast (c) images. Scale bar: 20 μm .

Treatment of HeLa cells with dye **1** resulted in a concentration dependant decrease of the red/green fluorescence intensity which implies a decrease in mitochondrial membrane potential (Fig. 4). Treatment of cells with 1 μM of dye **1** and 100 μM CCCP²⁴ a compound which completely depolarizes mitochondria resulted in noticeable decrease in mitochondrial membrane potential. These results shows that dye **1** depolarizes mitochondria in a concentration dependant manner.

The cytotoxicity of the synthesized dyes **4** and **1** were determined in HeLa cell lines using CCK-8 assay and compared to commercially available mitochondrial stain MitoTracker DeepRed (Table 2). All dyes were cytotoxic in a time dependant manner. The IC_{50} of dye **1** is 2.2 μM at 25 h which is comparable to MitoTracker DeepRed which has an IC_{50} of 2 μM at 25 h.

Dye **1**, which is a combination of heptamethine cyanine dye IR-786 **4** and a FDA approved drug Amoxapine **5** shows good photophysical properties in ethanol and selective staining of

Table 2
Cytotoxicity of dyes at different time points.

Dyes	IC_{50} (μM) at 4 h	IC_{50} (μM) at 19 h	IC_{50} (μM) at 25 h
IR-786	18	6.7	5.6
Dye-1	6.6	2.3	2.2
MitoTracker Deep Red	4	2.0	2.0

mitochondria in HeLa cells. This work paves way for future exploration of similar synergistic drug-dye combinations with improved photophysical properties and organelle selectivity. Improving the aqueous solubility of the drug-dye system and utility of such systems to support drug discovery efforts will be investigated further.

Acknowledgment

We thank Dr Adrian Blaser for the proton and carbon NMR, Dr Yuichiro Ueno for advice with quantum yield measurements, Sisira Kumara for the analytical HPLC, Sree Sreebhavan for high resolution mass spectra. We thank the Auckland Cancer Society Research Centre for financial support.

A. Supplementary data

Supplementary data associated with this article can be found, in the online version, at <https://doi.org/10.1016/j.bmcl.2018.05.001>.

References

- Zhu H, Fan J, Du J, Peng X. *Acc Chem Res.* 2016;49:2115–2126.
- Chen X, Bi Y, Wang T, et al. *Sci Rep.* 2015;5:1–10.
- Zhang H, Fan J, Wang J, Zhang S, Dou B, Peng X. *J Am Chem Soc.* 2013;135:11663–11669.
- Jose J, Loudet A, Ueno Y, Barhoumi R, Burghardt RC, Burgess K. *Org Biomol Chem.* 2010;8:2052–2059.
- Sharma A, Umar S, Kar P, Singh K, Sachdev M, Goel A. *Analyst.* 2016;141:137–143.
- Duchen MR, Szabadkai G. *Essays Biochem.* 2010;47:115–137.
- Nsiah-Sefaa A, McKenzie M. *Biosci Rep.* 2016;36:1–19.
- Tuppen HA, Blakely EL, Turnbull DM, Taylor RW. *Biochim Biophys Acta.* 2010;1797:113–128.

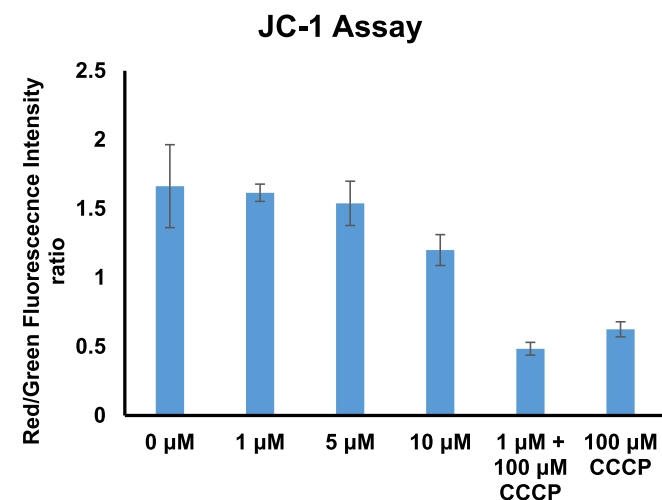


Figure 4. JC-1 assay showing dye **1** depolarizes mitochondrial membrane potential in a concentration dependant manner.

9. Sun W, Guo S, Hu C, Fan J, Peng X. *Chem Rev.* 2016;116:7768–7817.
10. Shi C, Wu JB, Pan D. *J Biomed Opt.* 2016;21:1–11.
11. Lee H, Mason JC, Achilefu S. *J Org Chem.* 2006;71:7862–7865.
12. Myochin T, Kiyose K, Hanaoka K, Kojima H, Terai T, Nagano T. *J Am Chem Soc.* 2011;133:3401–3409.
13. Zhang C, Tan X, Tan L, et al. *Cell Transplant.* 2011;20:741–751.
14. Dasari M, Lee S, Sy J, et al. *Org Lett.* 2010;12:3300–3303.
15. Vries EGE, Jong S, Gietema JA. *J Clin Oncol.* 2015;33:2585–2587.
16. Vernall AJ, Hill SJ, Kellam B. *Br J Pharmacol.* 2014;171:1073–1084.
17. Pankevich DE, Altevogt BM, Dunlop J, Gage FH, Hyman SE. *Neuron.* 2014;84:546–553.
18. Lydiard RB, Gelenberg AJ. *Pharmacotherapy.* 1981;1:163–178.
19. Kong R, Liu T, Zhu X, et al. *Clin Cancer Res.* 2014;20:3521–3530.
20. Robertson AM, Ferguson LR, Coopers GJS. *Toxicol Appl Pharmacol.* 1988;93:118–126.
21. Gallaher DL, Johnson ME. *The Analyst.* 1999;124:1541–1546.
22. Ueno Y, Jose J, Loudet A, Perez-Bolivar C, Anzenbacher P Jr., Burgess K. *J Am Chem Soc* 2011;133:51–55.
23. Smiley ST, Reers M, Mottola-Hartshorn M, et al. *Proc Natl Acad Sci USA.* 1991;88:3671–3675.
24. Lim MLR, Minamikawa T, Nagley P. *FEBS Lett.* 2001;503:69–74.